Sidewall Indentation and Buckling
of Deformed Aluminum Beverage Cans

Robert W. Bielenberg
Graduate Research Assistant, University of Nebraska-Lincoln

Scott H. Magner
Graduate Research Assistant, University of Nebraska-Lincoln

John D. Reid
Associate Professor, University of Nebraska-Lincoln
Mechanical Engineering Department
N104 WSEC (0656)
Lincoln, NE 68588
(402) 472-3084
jreid@unl.edu

ABSTRACT

Previous research has demonstrated that finite element analysis can be used to predict the structural behavior of aluminum beverage cans including the buckling of the sidewall of the can. Buckling of a beverage container can occur when the lid is pressed on dented cans during assembly. The purpose of this research was to simulate the sidewall indentation and the buckling of aluminum cans with a deformed sidewall using LS-DYNA and validate the results through physical testing. Simulation of the sidewall indentation was done with an impacting sphere. Parameters investigated through simulation included the size of the impacting sphere, velocity of sphere, and impact height along sidewall of can. Results from this study are maximum and final can deflection, maximum and final energy absorbed by the can, and force deflection data. Simulation of the buckling of the deformed can was also performed. Results from the deformed can buckling model compared well with physical testing based on buckled geometry, buckling load, and external work to buckle. The deformed can model proved capable of accurately simulating the buckling of the deformed can.

INTRODUCTION

The annual production of aluminum cans in the United States has reached approximately 100 billion cans per year. Production of such an enormous number of cans means that any small improvement in the manufacturing process results in large degrees of savings for the industry in terms of both time and money.

Recently, a potential production problem has been identified in the manufacture of aluminum cans. The problem arises when the cans are dented during the assembly process. As the cans move through the assembly process, they often impact the sides of the conveyor system and other objects producing small dents in the sidewall of the can. When the deformed can reaches the stage of assembly where the lid is pressed on, the weakened sidewall of the can may cause the can to buckle under the force of the press. A previous study completed by Robert Dick of the Aluminum Company of America (Alcoa) used finite element analysis to successfully simulate the buckling of aluminum cans under axial loading conditions (all references). However, combined analysis of the sidewall indentation and the buckling of a can with a deformed sidewall was not investigated.

The aim of this research was to simulate sidewall indentation and buckling of an aluminum can using LS-DYNA finite element analysis software and compare the results of the simulations with physical testing of the same event. LS-DYNA is a transient, nonlinear finite element analysis program that uses explicit time integration (Hallquist, 1997). Successful modeling of the buckling of the deformed can will provide a means of analysis of the effect of dent location and size on the buckling problem as well as possible redevelopment and improvement of the lid pressing process.

The investigation of the buckling of deformed aluminum cans consisted of three major parts. First, the necessary finite element models were developed to simulate the indentation and buckling of a deformed can in LS-DYNA. The second stage was the physical testing of the buckling of deformed aluminum cans. Finally, the physical test data was analyzed and compared with the results of the LS-DYNA simulation. These stages are discussed in detail in the following sections. The simulation effort was divided into two parts : (1) simulation of the indentation of the can sidewall and (2) simulation of the buckling of the dented aluminum can.

SIMULATION AND ANALYSIS OF SIDEWALL INDENTATION

The model developed to study the impact properties of the can sidewall was based on a model by Robert Dick of Alcoa. Vertical symmetry was used to reduce the size of the model to save computational time. Symmetric constraints were created by restricting all the nodes on the symmetry plane from translation perpendicular to the symmetry plane and rotation in the plane of symmetry. The can was made from shell elements placed on a floor of rigid shell elements and supported at the back by a wall of rigid shell elements. An impacting sphere was modeled with solid elements and located 0.254 mm from the center of the can. Model geometry is shown in Figure 1.
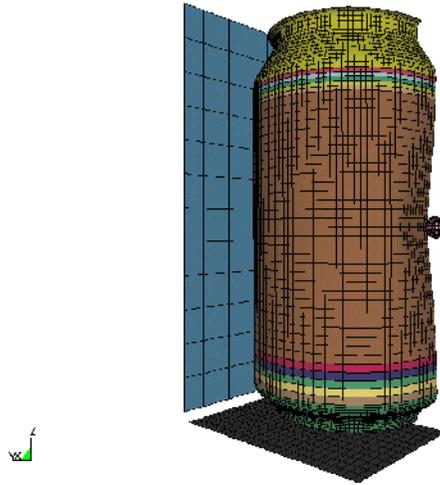
Figure 1. Sidewall Indentation Model - Post Impact

The aluminum can was divided into three parts: top, middle, and bottom. The top consisted of the portion of the can from the top of the sidewall to the top of the can.   The middle portion was defined as the flat sidewall. The portion of the can from the bottom of the sidewall to the bottom of the can was the bottom.   Transition regions consisting of the first five rows of elements at top and bottom of the middle part of the can accounted for thickness variations between the three parts. Thickness of shell elements for the top was set to 0.14732 mm, the middle 0.09652 mm, and the bottom 0.254 mm. Each of the five rows of transition elements stepped the thickness linearly between the two parts.

Once geometry considerations were taken care of, initial conditions were considered. First, gravity was added globally to the system. Second, an initial velocity was applied to the sphere. Simulation output was collected to gather the can deflection, energy absorbed, and force deflection data.

Sidewall Indentation Simulation
The parameters varied in this study included: initial sphere velocity, size of sphere, and location of impact along the sidewall of the can. Each parameter was investigated using a set of runs to vary the parameter while holding the rest constant. Each run was designated by

sphere diameter, initial velocity of the sphere and placement from center of can sidewall in positive z-direction. The simulation runs completed for the study are shown in Table 1.

Table 1. Simulation Runs for Indentation Parameter Study

Initial Velocity - 12.7 mm sphere impact at center of can	
run 1	initial velocity 2540.0 mm/s
run 2	initial velocity 2857.5 mm/s
run 3	initial velocity 3175.0 mm/s
run 4	initial velocity 3492.5 mm/s
run 5	initial velocity 3810.0 mm/s
Sphere Size – 6.35 mm and 19.05 mm at varied speeds (sphere mass constant)	
run 6	sphere 6.35 mm, initial velocity 2540.0 mm/s
run 7	sphere 6.35 mm, initial velocity 3175.0 mm/s
run 8	sphere 6.35 mm, initial velocity 3810.0 mm/s
run 9	sphere 19.05 mm, initial velocity 2540.0 mm/s
run 10	sphere 19.05 mm, initial velocity 3175.0 mm/s
run 11	sphere 19.05 mm, initial velocity 3810.0 mm/s
Impact Height – 12.7 mm sphere at 3175 mm/s along varied sidewall heights	
run 12	impact at 46.7 mm from center of can
run 13	impact at 23.35 mm from center of can
run 14	impact at -23.35 mm from center of can
run 15	impact at -46.7 mm from center of can

Results
Can deflection, energy absorption, and force-deflection information for all sidewall indentation simulations are listed in Table 2. The can simulation end was reached when the can sidewall was finished rebounding from the sphere impact and the final deflection was reached.

Table 2. Beverage Can Sidewall Impact Results

Initial Velocity (mm/s)	Can Deflection		Energy Absorbed	Force Deflection Information	
	Max (mm)	Final (mm)	Final (N-mm)	Peak Force (N)	Loading Stiffness (N/mm)*
sphere diameter = 12.7 mm					
2540	5.3	0.1	3.1	4.8	0.72
2858	5.9	3.0	10.3	5.7	0.78
3175	6.4	4.0	13.0	6.5	0.84
3493	7.0	4.4	15.7	7.3	0.94
3810	7.5	4.8	19.8	8.0	0.84
sphere diameter = 6.35 mm					
2540	5.2	0.1	3.1	4.9	0.78
3175	6.4	4.0	12.9	6.5	0.88
3810	7.5	4.9	19.2	8.0	0.90
sphere diameter = 19.05 mm					
2540	5.2	0.1	3.0	4.8	0.76
3175	6.4	3.9	12.8	6.5	0.87
3810	7.5	4.8	19.1	8.0	0.89
Impact height**	sphere diameter = 12.7 mm, initial velocity = 3175 mm/s				
50 mm	3.7	0.4	3.9	10.8	NA
25 mm	6.3	3.4	10.8	6.4	0.77
-25 mm	5.8	4.0	14.4	7.8	1.08
-50 mm	1.3	0.3	7.9	20.8	NA

* Quantity was estimated from a plot.
** Impact height is measured from the center of the sidewall of the can.
NA - Not Available

Can Deflection/Indentation. The change in can deflection with increased initial velocity is graphed in Figure 2. All initial velocities greater than 2540 mm/s resulted in permanent deformation of the can while an initial velocity of 2540 mm/s resulted in an elastic rebound. A linear relationship is seen between increasing initial velocity of the sphere and maximum can deflection, while the relationship between final can deflection and increasing initial velocity is parabolic in nature. At an initial velocity of 2540 mm/s, the can indented 5.3 mm and rebounded. The maximum can deflection was reached at 3810 mm/s, the maximum velocity tested. A deflection of 7.5 mm was produced and rebounded to 4.8 mm. Can deflection was not affected by sphere size. Both the 6.35 mm and 19.05 mm spheres deflected the can the same as the 12.7 mm sphere. Deflection of the can changed only with respect to changes in initial velocity.

Can deflection as a function of impact height is also graphed in Figure 2. The largest maximum deflection was achieved at the center of the sidewall. Smaller maximum deflections were found as the impact point moved nearer to the ends of the can sidewall. Final deflection of the can

demonstrates a similar trend, except that the largest final deflection was not found at the middle of the sidewall. Instead, the largest final deflection is found at 23.35 mm below the center of the can.
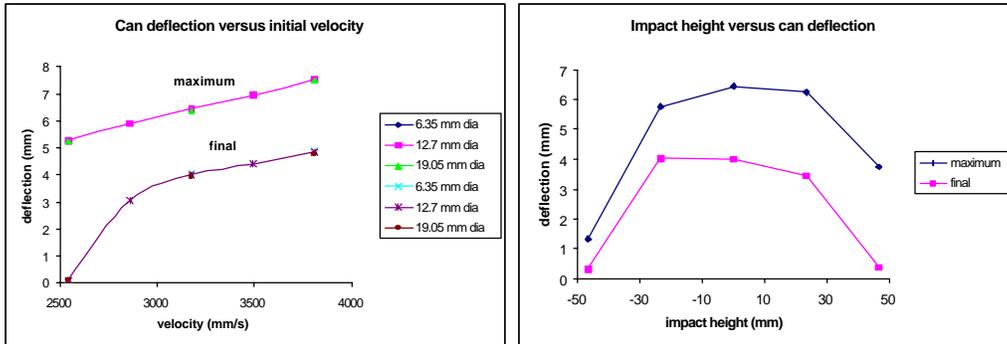
Figure 2. Deflection - Sidewall Indentation

Energy absorbed. The energy absorbed by the can during impact with the sphere is shown in Figure 3. Energy absorbed is plotted against the initial velocity and the impact height of the sphere. It should be noted that the data obtained for energy absorbed is for a half can model and reflects only half the amount of energy that would be absorbed by a full can. Both figures show similar trends as the deflection curves discussed above. Maximum energy absorbed and final energy absorbed increased with increasing velocity. It can be seen from the data for impact height versus can deflection that the highest maximum energy was found at the center of the can. The final energy absorbed was directly related to the final deflection of the can.   Therefore, final energy absorbed was highest for an impact 23.35 mm below the center of the can. Once again, sphere size appeared to have no effect on the energy absorbed for either the initial velocity or impact height cases.
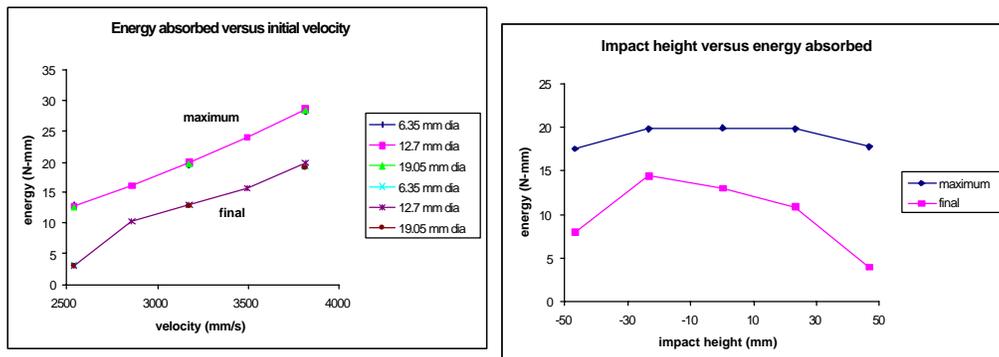
Figure 3. Energy Absorption - Sidewall Indentation

Force deflection data. The force data collected from the sidewall indentation model is shown in Figure 4. Maximum impact force increased linearly as a function of initial velocity. A maximum force of 8.01 N was achieved for the 3810 mm/s run, while the 2540 mm/s run resulted in a maximum force of about 4.89 N. Maximum force as a function of impact height is also plotted in Figure 4 and shows that smallest forces were encountered at the center of the can, while maximum forces were achieved at negative impact height values. Once again it should be noted

that forces obtained are for a half can model only and reflect half of what the value would be on a full can.
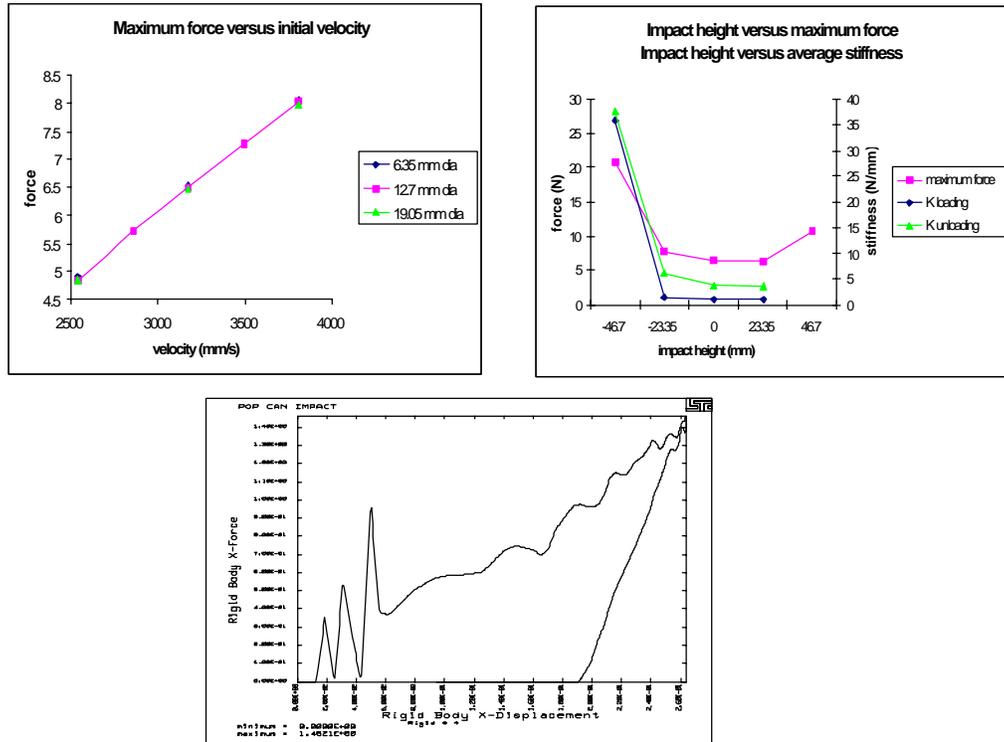
Figure 4. Forces - Sidewall Indentation

Force deflection properties of the can during impact were also investigated. This was accomplished by cross plotting the acceleration of the sphere scaled by its mass with the x-displacement of the sphere. This data was then used to determine the loading and unloading stiffness of the cans during impact. The slope was calculated by estimating the slope during indentation and rebound. Force deflection curves for a 12.7mm sphere impacting the center of the can at 3175 mm/s are shown in Figure 4. The stiffness (K) is shown as a function of impact height. For impacts at the center of the can, the loading and unloading stiffness were approximately constant at about 0.84 and 3.33 N/mm, respectively. Sphere size did not affect maximum force or stiffness.

Effect of Parameter Variation
The parameters varied in the sidewall indentation study were the initial velocity, the sphere size, and the impact height on the can. Changing the initial velocity of the impacting sphere appears to be directly proportional to maximum can deflection, energy absorbed, and maximum force. Creation of a permanent dent in the can sidewall was dependent on initial velocity as well. The cutoff velocity needed for formation of a permanent dent instead of elastic rebound is in the range of 2540 to 2857.5 mm/s.

Changing the sphere size had a negligible effect in this study. This was primarily due to the fact that the density of the different sized spheres was altered to maintain constant mass among the various sphere sizes. The results indicate that for the range chosen (6.35 to 19.05 mm diameter)

objects of spherical geometry and similar mass will have the same effects on the parameters studied.

Effects of varying the impact height along the length of the sidewall were very significant. Maximum deflection and energy absorption occurred at the center of the sidewall while it was significantly less at the top and bottom of the sidewall. Greater deflection occurred at the top of the sidewall as opposed to the bottom primarily because of the difference in thickness, with the top being thinner than the bottom. Data from the initial velocity parameter study would indicate that a large final deflection should result in a large final energy absorption. This was also true with respect to the impact height parameter. The larger final deflections led to higher final energy being absorbed. The largest value for the final energy absorbed by the can as a function of impact height was 14.406 N-mm at 23.35 mm from the center of the can. The maximum energy absorbed during indentation should be, and was, the same for all of the impacts because the sphere velocity was not changed. In other words, the initial kinetic energy of the sphere is transferred to the can upon impact, independent of impact height.

DEFORMED CAN BUCKLING MODEL

A second model was developed to analyze the buckling of a can with a dented sidewall under a compressive load. In order to create the buckling model, the can sidewall indentation model was modified. The model was based on the one half can model developed previously. Elements of the half can model were reflected to create a full model of the can. Three different cross sections were combined in the can model; the top, the middle, and the bottom. There are also five rows of elements with varying thickness between each of these parts that model the transition of the wall thickness between the major sections. All of the sections of the can were modeled using shell elements with the Belytschko-Wong-Chiang element formulation. A linearly plastic material was used to model the aluminum material for the can. The model of the can was impacted at the middle of the sidewall of the can by a 6.35 mm rigid sphere with a velocity of 2540 mm/s. Two rigid walls support the can.

The full can model was simulated successfully with the sphere impact creating a permanent dent in the sidewall of the can of 6.05 mm. Deformed geometry from the full model of the sidewall indentation was exported from LS-TAURUS and used as the base geometry for the can in the buckling model. A lid was then added to the top of the can to comply with the physical tests and the sphere and the rigid sidewall supporting the can were removed. A rigid disk was added above the can to simulate the press and was given a prescribed motion 127 mm downward in order to buckle the can. Speed of the lid press was set at 211.58 mm/s in order to match the physical test set up. The model can be seen in Figure 5.

Figure 5. Deformed Can Buckling Model - Initial Condition

10 - 34

Results from the buckling simulation are compared to physical testing in a later section of this paper.

PHYSICAL TESTING

Physical Testing of the indentation and buckling of the aluminum cans was required to validate the LS-DYNA models and to give confidence in the analysis of the results. To this end, a set of cans were dented similarly to the simulation, and then buckled under loading comparable to the LS-DYNA simulations.

Indentation of Cans
The results of the physical tests and the final model could not be compared accurately unless the cans had the same deformation. A can denting device was built that dented the cans using a . 6.35 mm diameter sphere that dropped onto the middle of the cans at the same velocity as the LS-DYNA simulation. A schematic of the device can be seen in Figure 6.
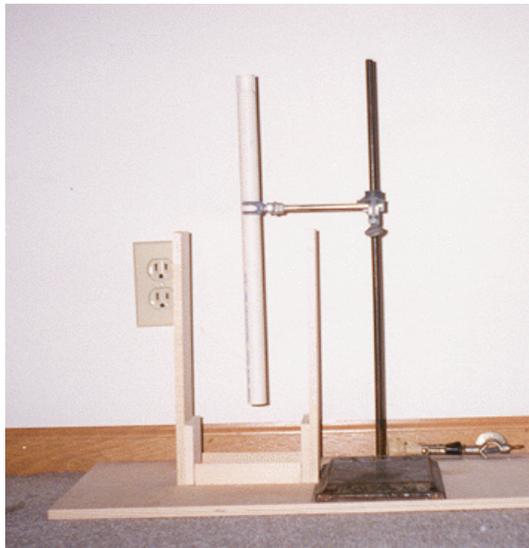
Figure 6. Can Denting Device

The device consists of a wooden base and frame that holds the can in place, a metal sphere, and a suspended PVC pipe that controlled the velocity and location of the sphere impact. The impact was centered over the middle of the can. The velocity of the impact was determined by the height of the sphere drop. The height from which the sphere was dropped was calculated using basic physics to be 406.4 mm. This height produced a sphere velocity identical to the simulation sphere impact. A set of fifteen cans was dented using the device and readied for the buckling tests.

Buckling of Cans
The second stage of the physical testing involved buckling both deformed and undeformed aluminum cans under a compressive load. The buckling of the cans was performed using the Mechanical Testing System (MTS) machine at the Mechanical Engineering Department at the University of Nebraska, Lincoln. The MTS machine has the ability to test mechanical specimens under a wide variety of loading conditions and output the test data into computer files for manipulation. For the buckling of the aluminum cans, the MTS machine was set to replicate the loading conditions used in the LS-DYNA simulation. It was set to compress the cans 12.7 mm at a velocity of 212 mm/s. The MTS machine output the force and displacement of the can

buckling every 0.0002 seconds. The physical test setup using the MTS machine is shown in Figure 7.

Figure 7. Can Buckling Device

The MTS machine was used to bucklefifteen deformed aluminum cans. The force displacement data output from the machine was analyzed. Table 3 summarizes the results of the physical buckling tests. The results of the physical tests are compared with the LS-DYNA simulation output in the following section.

Table 3. Physical Testing Results for Deformed Cans

Can Test No.	Buckling Load (N)	Displacement at Initial Buckle (mm)
1	-663	-1.37
2	-694	-1.37
3	-635	-1.57
4	-985	-1.55
5	-930	-1.52
6	-761	-1.34
7	-988	-1.59
8	-853	-1.34
9	-856	-1.31
10	-798	-1.34
11	-884	-1.48
12	-884	-1.48
13	-694	-1.30
14	-961	-1.49
15	-645	-1.30
Average Buckling load/displacement	-815	-1.42

ANALYSIS AND COMPARISON

The results of the deformed can buckling computer simulations and the physical testing were compared in order to test the accuracy and validity of the LS-DYNA model. The results of the simulation and testing were compared based on buckled geometry, buckling load, and external work to buckle.

Deformed Can Buckling
The LS-DYNA model of the buckling of a deformed aluminum can was compared with physical test data based on buckled geometry, buckling load, and external work to buckle. The buckled geometry of the can from the LS-DYNA simulation and the physical testing can be seen in Figure 8. The buckling mode of the simulation and the physical test are very similar. The buckling of the deformed can caves in around the indentation in the sidewall of the can pushing the sides adjacent to the dented face to deform outward. The side of the can then buckles along the line of the dent as well as smaller areas on the opposite side of the dent dimples. The buckling of the deformed cans is very close to the physical test because the dent in the cans forces the buckling to occur at that location due to stress concentrations. The DYNA model has no other imperfections that would promote other buckling modes as in an actual can.

Figure 8. Buckled Deformed Aluminum Can

The buckling load curves and the external work curves of the deformed can simulation also compare well with the results of the physical testing. The average buckling load of the testing was 815.44 N while the LS-DYNA model predicted a slightly higher 871.85 N. The simulation load was slightly higher due to the higher stiffness of the finite elements as compared to the actual can material and the small imperfections and thickness variations in the test can that are not present in the model. It should also be noted that the cans tested were not Alcoa cans like the model and may have had slight design differences. The comparison of the force-displacement curves is shown in Figure 9. The buckling force curves for both cases follow a very similar trend. The simulation predicts the buckling at a larger displacement than the testing showed. This may be due to press setup procedure in the testing. The external work curves shown in Figure 10 also show nearly identical results between the simulation and the physical testing. The curves follow a similar trend and have very close final energy levels. The

similarity in the results of the geometry, force, and energy data would suggest that the LS-DYNA simulation of the deformed cans is quite accurate.

Force displacement curve comparison of LS-DYNA simulation and physical testing of the buckling of a deformed aluminum can
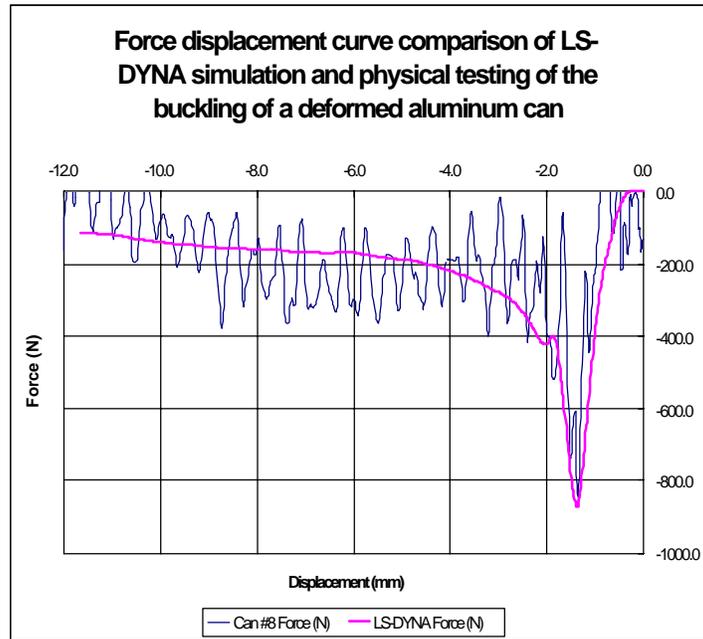
Figure 9. Buckling Force-Displacement

Graph of external work for LS-DYNA simulation and physical testing of deformed aluminum cans
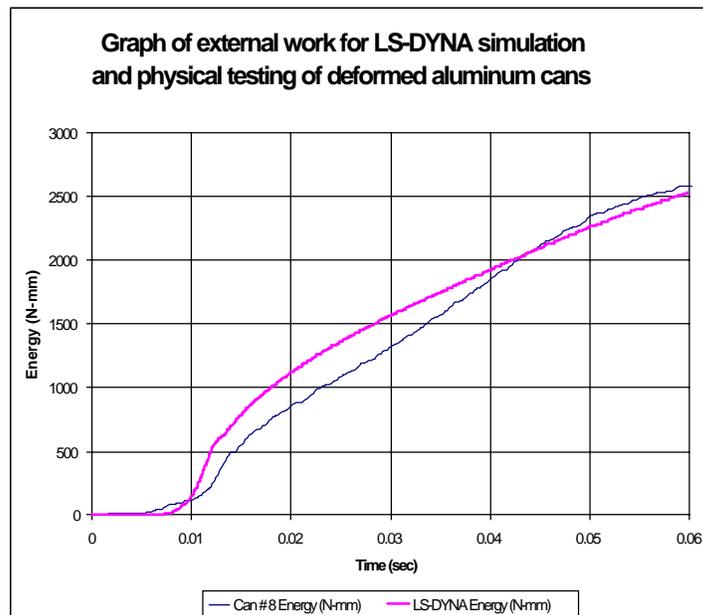
Figure 10. Buckling Energy Curves

CONCLUSIONS AND RECOMMENDATIONS

The study of the buckling of deformed aluminum cans using LS-DYNA lead to several conclusions and recommendations. First, the sidewall indentation model showed that changes in the parameters studied have a definite influence on the side impact properties of aluminum beverage cans. The finite element model developed provides a good means to determine and quantify these effects with respect to the sidewall. The parameter study found that the velocity of the impact and the location of the impact on the can have the greatest affect on the indentation of the can. The baseline model provides for expansion of the parameter study to investigate the changes in can performance as a function of wall thickness.

The deformed can model can be used to predict the buckling of deformed aluminum cans under a compressive load. The deformed shape of the simulation and the physical tests were very similar. The buckling load and energy curves were also very similar.

The development of a successful deformed can buckling model left room for further development and improvement. The physical testing could be improved by increasing the number of tests and obtaining actual Alcoa cans for testing. Additional buckling models could be made to predict the effect of different dent sizes and locations. A more complex press model that more accurately simulates the lid pressing operation may improve simulation results.

ACKNOWLEDGMENTS

REFERENCES

Bhakuni, N.D. (1990). Structural Optimization of Beverage Cans, Ohio State University Master s Thesis, 1990 December.

Bhakuni, N.D. (1989). CAD/FEM Interface for Beverage Containers and Other Shells of Revolution, Alcoa Laboratories Report No.57-89-23, 1989.

Biondich, S.C., and Dick R.E. (1990).   A New Reformed Shell Forming Process, Transactions of the North American Manufacturing Research Institution of SME, 1990, pp. 33-40.

Dick, R.E. (1994).   Axial Buckling of Beverage Can Sidewalls, 2nd International LS-DYNA3D Conference, Westin, St. Francis, San Francisco, 20-21 September 1994, Paper No. 21LSD3D103.

Dick, R.E., Smith, G.L., and Myers, G.L . (1992).   Aluminum Beverage Cans with Improved Drop Resistance, presented at the SME International Can Manufacturing Technology Clinic, Rosemont, Il., 30 September-3 October 1992.

Dick, R.E. (1991).   MESHG2- An Improved Mesh Generator of Shells of Revolution, Alcoa Laboratories Report No.57-91-23, 1991.

Dick, R.E. (1987).   MESHGEN - A Two- and Three-Dimensional Mesh Generator for Use with the ABAQUS and MARC Finite Element Codes, Alcoa Laboratories Report No. 57-87-12, 1987.

Hallquist, J.O. (1997). *LS-DYNA Keyword Users Manual : Version 940*, Livermore California, Livermore Software Technology Corporation, June 1997.

Trageser, A.B., and Dick, R.E. (1991).   Beverage Can Structural Analysis and Automation, presented at the Design Productivity International Conference, Honolulu, Ha., 3-9 February 1991.

Trageser, A.B., and Dick, R.E. (1988).   Aluminum Can Design Using Finite Element Methods, presented at the SME Can Manufacturing Technical Symposium, Schaumburg, Il., 14-16 September 1988.